C. R. Physique ••• (••••) •••–•••

Contents lists available at ScienceDirect

Comptes Rendus Physique

www.sciencedirect.com

From statistical physics to social sciences / *De la physique statistique aux sciences sociales*

Reality-inspired voter models: A mini-review

Modèles d'électeurs inspirés de la réalité : une mini-revue

Sidney Redner

Santa Fe Institute, 1399 Hyde Park Road, Santa Fe, NM 87501, USA

ARTICLE INFO

Article history:
Available online xxxx

Keywords:
Voter model
Heterogeneity
Networks
Non-conserved dynamics
Majority rule
Multiple states

Mots-clés :
Modèle de l'électeur
Hétérogénéité
Réseaux
Dynamique non conservée
Règle de la majorité
États multiples

ABSTRACT

This mini-review presents extensions of the voter model that incorporate various plausible features of real decision-making processes by individuals. Although these generalizations are not calibrated by empirical data, the resulting dynamics are suggestive of realistic collective social behaviors.

RÉSUMÉ

Cette mini-revue présente des extensions du modèle de l'électeur qui intègrent divers éléments plausibles des processus réels de prise de décision par des individus. Bien que ces généralisations ne soient pas calibrées par des données empiriques, la dynamique qui en résulte suggère des comportements sociaux collectifs réalistes.

1. Introduction

The voter model (VM) is an idealized description for the evolution of opinions in a population. Each individual (or voter) can assume one of two states (e.g., **1**/**0**, ↑ / ↓, Democrat/Republican), and a single voter resides at each node of an arbitrary network. A voter is selected at random and adopts the state of a randomly chosen neighboring voter. Each individual is influenced only by a fixed set of neighbors; there is no notion of a "right" or a "wrong" opinion, there are no external influences (e.g., news media), or other types of interactions. The basic update step is repeated at unit rate until a population of N agents necessarily reaches consensus; this inevitability of consensus is one of the basic features of the VM.

The simplicity and utility of the VM has sparked much research in probability theory [1–4] and statistical physics [5–10] to understand its dynamical behavior. One of the appeals of the VM is that it is exactly soluble when voters are situated on regular lattices or homogeneous graphs. However, it is hard to envision that a large group of individuals can come to consensus on anything. This dichotomy between eventual consensus in the VM and the common experience of opinion diversity has motivated generalizations of the VM to include realistic aspects of opinion formation that can forestall consensus. Ex-

E-mail address: redner@santafe.edu.

https://doi.org/10.1016/j.crhy.2019.05.004
1631-0705/

Please cite this article in press as: S. Redner, Reality-inspired voter models: A mini-review, C. R. Physique (2019), https://doi.org/10.1016/j.crhy.2019.05.004

amples include individual stubbornness, partisanship, truth versus falsehood, individual heterogeneity, social heterogeneity, and multiple opinion states.

Some of these extensions of the VM are reviewed in this article; a recent review that has some overlap with the topics discussed here is Ref. [11]. Unless stated otherwise, the underlying social network is a complete graph of N nodes. While obviously unrealistic, this geometry-free setting gives rise to much interesting phenomenology. Additionally, real social networks are long ranged [12–14], so the complete graph may be a better approximation than a regular lattice for the underlying social substrate. What is not treated here is the possibility of changes in that social substrate at the same time that individual opinions are changing. For a discussion of such adaptive voter models see, e.g., Refs. [15–21].

The focus of this article is primarily on topics that have been addressed by my collaborators and myself; space limitations prevent a fuller discussion of many important developments in this field. While the social attributes mentioned above are inspired by reality, the resulting models should still not be viewed as realistic. What is missing is a calibration of the parameters of these more general models with real social data [22]. In the absence of such a connection, these extensions of the VM might be viewed as instructive theoretical games. Nevertheless, they are phenomenologically rich and perhaps hint at how to construct realistic opinion dynamics models.

2. Classic voter model

In the classic VM, N voters live at the nodes of an arbitrary static graph, with one voter per node. The opinion evolution is simplicity itself (Fig. 1):

1. pick a voter uniformly at random;
2. this voter adopts the state of a random neighbor;
3. repeat 1 & 2 until consensus is necessarily reached.

Figuratively, each agent has no self-confidence and merely adopts the state of one of its neighbors. Two basic observables of the VM are: (i) the *exit probability* $E(m)$ that N voters reach $\uparrow$ consensus as a function of the initial magnetization $m \equiv (N_\uparrow - N_\downarrow)/N$, where $N_\uparrow$ and $N_\downarrow$ are the initial number of $\uparrow$ and $\downarrow$ voters, respectively, and (ii) the *consensus time* $T(m)$, the average time to reach consensus as a function of m. For notational simplicity, the N dependence is not written for $E(m)$ and $T(m)$.

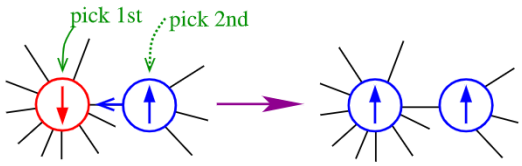

Fig. 1. Voter model update rule on a graph: a random voter is picked and adopts the state of a random neighbor.

To mathematically express the update rule on a homogeneous graph, let $\sigma_i = \pm 1$ denote the voter state at site i. It is easy to check that the rate w_i at which this voter state σ_i changes is given by

$$w_i = \frac{1}{2}\left(1 - \frac{\sigma_i}{z}\sum_j \sigma_j\right) \tag{1}$$

where z is the coordination number of each node and the sum runs over the j nearest neighbors of site i. A crucial feature of this transition rate is its linearity in the number of disagreeing neighbors. This linearity underlies the solvability of the voter model. Another important consequence of linearity is that there is no surface tension along an interface that separates domains of $\uparrow$ and $\downarrow$ voters on finite-dimensional lattices. Here, surface tension means that the interaction tends to make same-opinion clusters compact and therefore hard to break. Thus the voter model has a different character than the kinetic Ising model with single spin-flip dynamics, in which interface motion is driven by surface tension [7,9,23,24].

Using (1) is immediate to verify that the average magnetization, $m \equiv \sum_i \langle \sigma_i \rangle / N$, is conserved. Here $\langle \cdot \rangle$ indicates the average of the quantity within the angle brackets over all realizations of the dynamics. The time evolution of the average of σ_i is given by

$$\langle \dot{\sigma}_i \rangle = -2\langle \sigma_i w_i \rangle \tag{2a}$$

because whenever a voter flips, with rate w_i, the change in the value of the voter's state is $-2\sigma_i$. Substituting the flip rate (1) into the above equation gives

$$\langle \dot{\sigma}_i \rangle = -\langle \sigma_i \rangle + \frac{1}{z}\sum_j \langle \sigma_j \rangle \tag{2b}$$

Please cite this article in press as: S. Redner, Reality-inspired voter models: A mini-review, C. R. Physique (2019), https://doi.org/10.1016/j.crhy.2019.05.004

where we use the fact that $\sigma_i^2 = 1$. Summing (2b) over all sites i gives magnetization conservation, $\dot{m} = 0$.

This conservation law immediately determines the exit probability. When the initial magnetization equals m, the average value of the final magnetization when consensus is eventually reached equals

$$\langle m_\infty \rangle = 1 \times E(m) + (-1) \times \big(1 - E(m)\big) \tag{3}$$

That is, a final magnetization $+1$ is reached with probability $E(m)$, while $m_\infty = -1$ is reached with probability $1 - E(m)$. Since $\langle m_\infty \rangle = m$ by magnetization conservation, we have $E(m) = \frac{1}{2}(1+m)$.

There is a systematic tool with many applications to first-passage processes [25–27]—the backward Kolmogorov equation—that can be used to determine both the exit probability and the consensus time in a simple way. We will use this formalism throughout this article. Suppose that the density of $\uparrow$ voters equals ρ. After a single update, ρ may change to $\rho \pm \delta\rho$ or remain the same, with respective probabilities $w_{\rho\to\rho\pm\delta\rho}$ and $w_{\rho\to\rho}$, after which the process restarts. Accordingly, the exit probability obeys the backward Kolmogorov equation

$$E(\rho) = w_{\rho\to\rho+\delta\rho} E(\rho+\delta\rho) + w_{\rho\to\rho-\delta\rho} E(\rho-\delta\rho) + w_{\rho\to\rho} E(\rho) \tag{4a}$$

subject to the boundary conditions $E(0) = 0$, $E(1) = 1$. For the VM, the flipping probabilities are $w_{\rho\to\rho\pm\delta\rho} = \rho(1-\rho)$ and $w_{\rho\to\rho} = 1 - 2\rho(1-\rho)$. Taking the continuum limit of (4a) gives $\mathrm{d}^2E/\mathrm{d}\rho^2 = 0$, with solution $E(\rho) = \rho$, or equivalently, $E(m) = \frac{1}{2}(1+m)$. It is purely a matter of convenience whether to use m or ρ as the dependent variable.

We obtain the time to reach either $\uparrow$ or $\downarrow$ consensus by the direct analog of Eq. (4a):

$$T(\rho) = w_{\rho\to\rho+\delta\rho}\big[T(\rho+\delta\rho) + \delta t\big] + w_{\rho\to\rho-\delta\rho}\big[T(\rho-\delta\rho) + \delta t\big] + w_{\rho\to\rho}\big[T(\rho) + \delta t\big] \tag{4b}$$

That is, the consensus time from an initial state with density ρ of $\uparrow$ voters equals the probability for an update to a new state where one voter has changed its opinion, multiplied by the time to reach consensus from this new state plus the time $\delta t = 1/N$ for a single update. The continuum limit now gives $N\rho(1-\rho)\,\mathrm{d}^2T/\mathrm{d}\rho^2 = -1$, subject to the boundary conditions $T(0) = T(1) = 0$. The solution is

$$T(\rho) = -N\big[(1-\rho)\ln(1-\rho) + \rho\ln\rho\big] \tag{5}$$

This linear N dependence also represents the generic behavior for the consensus time of the VM on Euclidean lattices in spatial dimensions $d \geq 3$. For $d = 2$, $T \sim N\ln N$, while for $d = 1$, $T \sim N^2$ [1–5].

3. Stubborn/confident voters

3.1. Individual heterogeneity

While each individual in the VM has no self confidence, real people do have some of this attribute, and it is natural to examine its role on VM dynamics. Self confidence can be viewed as quantifying the relative weights of individual versus social information. Other factors that influence the weights of these two information sources include: lower cost of individual versus social information, prestige or authority of an acquaintance, propensity for conformity, perceived differences in accuracy of individual versus social information, etc. Many of these issues have been explored in the social science literature (see, e.g., [28,29]).

Perhaps the simplest way to implement self confidence is to endow each voter i with its own intrinsic flip rate r_i [30]. That is, when a voter consults a neighbor with a different opinion, the voter changes state with rate r_i instead of with rate 1. Such a diversity of individual thresholds to a stimulus has been found to play an important role in controlling collective social behaviors [31–33]. The transition rate of voter i with intrinsic flip rate r_i in this *heterogeneous* voter model (HVM) now is (compare with Eq. (1))

$$w_i = \frac{1}{2}\Big(1 - \frac{r_i\sigma_i}{z}\sum_j \sigma_j\Big) \tag{6}$$

Following the same steps as in Eq. (2), we may verify that it is not the magnetization, but rather the inverse rate-weighted magnetization, $\omega \equiv \langle \sigma_i/r_i \rangle$, which is conserved. As a consequence, the probability for a population with initial value ω to reach $\uparrow$ consensus equals ω. Thus a small fraction of $\uparrow$ voters with very small flip rates—stubborn voters—leads to a probability of reaching $\uparrow$ consensus that can be arbitrarily close to 1, even if most of the population is initially in the $\downarrow$ state.

One can infer the average consensus time T for N heterogeneous voters on the complete graph by the following simple argument. For specificity, suppose that the flip rate distribution is $p(r) = A\,r^{-\alpha}$, with $r \in (0, r_{\max}]$ and $\alpha \in [0,1)$ so that $p(r)$ is normalizable. To compare across different α values, we fix the average flip rate of the population to be 1. These conditions give $r_{\max} = (2-\alpha)/(1-\alpha)$ and $A = (2-\alpha)r_{\max}^{\alpha-2}$.

Please cite this article in press as: S. Redner, Reality-inspired voter models: A mini-review, C. R. Physique (2019), https://doi.org/10.1016/j.crhy.2019.05.004

A voter with flip rate r needs to attempt of the order of $1/r$ flips before it actually changes state. Consequently, we can view the population as containing N/r effective voters. Since the consensus time of the VM is proportional to N, we anticipate that the consensus time in the HVM should be proportional to the average value of N/r. Also, as will be shown in Eq. (16), the consensus time of the voter model on a general complex graph is proportional to the effective population size. With this hypothesis, the consensus time in the HVM is $T \sim N\langle 1/r\rangle$. To determine $\langle 1/r\rangle$ for the flip-rate distribution $p(r) = Ar^{-\alpha}$, we first use the fact that the smallest rate $r_{\rm min}$ among a finite population of N voters is non-zero and determined by the extremal criterion [34]

$$\int_0^{r_{\rm min}} A\, r^{-\alpha}\, {\rm d}r = N^{-1}$$

i.e. one voter in a population of N has a flip rate $r_{\rm min}$ or smaller. This criterion gives $r_{\rm min} \sim N^{-1/(1-\alpha)}$. Now we estimate $\langle 1/r\rangle$ as

$$\langle 1/r\rangle = \int_0^{r_{\rm max}} \frac{p(r)}{r}\, {\rm d}r \sim \int_{r_{\rm min}}^{r_{\rm max}} \frac{p(r)}{r}\, {\rm d}r \sim N^{\alpha/(1-\alpha)}$$

Finally,

$$T \sim N^{1/(1-\alpha)} \tag{7}$$

for $0 < \alpha < 1$, while $T \sim N \ln N$ for $\alpha = 0$. Thus heterogeneity in individual flip rates forestalls consensus, as the consensus time scales superlinearly with N. Notice that the inverse rate of the stubbornest voters is the same order as the consensus time, so it is these stubbornest voters that control the approach to consensus. The phenomenon that a small fraction of stubborn individual can overcome the majority opinion has been studied both in the social science [35,36] and physics literatures [37,38], and begins to address the basic question of how can a small minority opinion group can eventually supplant a majority opinion.

3.2. Confident voting

The lack of individual voter confidence is one of many unrealistic aspects of the VM. There are a variety of socially/cognitively plausible mechanisms that people might use to solve the dilemma of how much weight to give to self knowledge compared to the knowledge of others when deciding what to believe or what to do. One such mechanism is reinforcement; in the context of the voter model, a voter night typically require multiple encounters with neighbors that hold a different opinion before the voter actually changes opinion. This feature was also highlighted in the social experiment of Centola [39], where individual behavior changed only when a person received multiple reinforcing inputs from others. Such threshold behavior also arises in the q-voter model [40] and in contagion models [41].

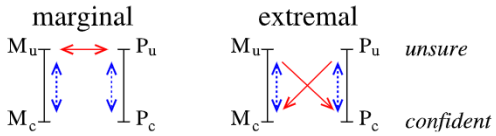

Fig. 2. Illustration of the (a) marginal, and (b) extremal confident voter models. Dashed arrows indicate possible confidence level changes, while solid arrows indicate possible opinion change events.

We investigate the role of a threshold through the *confident* voter model (CVM) [42], in which each voter has two opinion states and two levels of commitment to an opinion—confident and unsure. Upon interacting with an agent of a different opinion, a confident voter becomes unsure but keeps its opinion, while an unsure agent changes opinion. That is, a confident voter requires two consecutive prompts before changing opinion in the CVM (Fig. 2).

The basic variables are the opinion of each voter and its confidence level. We label the states of an agent as $P_{\rm c}$ and $P_{\rm u}$ for confident and unsure $\uparrow$ agents, respectively, and correspondingly $M_{\rm c}$ and $M_{\rm u}$ for $\downarrow$ agents. There are two natural variants of confident voting:

- *marginal:* an unsure agent that changes opinion is also unsure about the new opinion state and can switch back in a single update;
- *extremal:* an unsure agent "sees the light" after an opinion change and becomes confident of its opinion. This voter again requires two interactions with an opposite-opinion voter to switch another time.

Please cite this article in press as: S. Redner, Reality-inspired voter models: A mini-review, C. R. Physique (2019), https://doi.org/10.1016/j.crhy.2019.05.004

With the assumption that the rates of all processes sketched in Fig. 2 equal 1, it is simple exercise to write the rate equations for the densities of voters in each state. For the marginal version, these equations are:

Marginal:

$$\begin{aligned}\dot{P}_c &= -(M_c + M_u)P_c + P_cP_u \\ \dot{P}_u &= \ \ MP_c - P_cP_u + (M_uP_c - M_cP_u)\end{aligned} \tag{8a}$$

with parallel equations for M_c and M_u by interchanging $M \leftrightarrow P$. For the extremal version, the rate equations are (and similarly for M_c and M_u).

Extremal:

$$\begin{aligned}\dot{P}_c &= -M_cP_c + M_uP_u + P_cP_u \\ \dot{P}_u &= \ \ M_cP_c - M_uP_u - P_cP_u + (M_uP_c - M_cP_u)\end{aligned} \tag{8b}$$

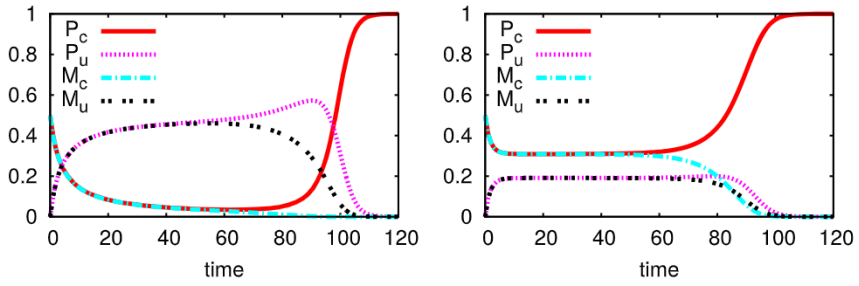

Fig. 3. Evolution of the densities for the marginal (left) and extremal (right) models with the near-symmetric initial condition $P_c = 0.50001$, $M_c = 0.49999$, and $P_u = M_u = 0$.

Solving these equations [42] gives the following basic results: for a symmetric population with equal densities of ↑ and ↓ voters, the final densities are $P_c = M_c = 0$ and $P_u = M_u = 1$ for the marginal model and $P_c = M_c = \frac{1}{2} - P_u = \frac{1}{2} - M_u = \frac{1}{4}(\sqrt{5}+1)$ for the extremal model. It is intriguing that for the extremal version of the CVM, a symmetric population does *not* reach consensus. However, for a slight asymmetry in the initial conditions, consensus is reached after a time scale that is of the order of $\ln N$. Intriguingly, the relaxation to consensus is governed by two widely separated time scales (Fig. 3). We will encounter another example of this multiple time-scale relaxation in a 3-state voter model with constrained voting rules in Sec. 6.1.

4. Heterogeneous networks

A fruitful extension of the voter model is to networks with broad distributions of degrees [43–49]; the degree of a node is the number of incident links on this node. Here, the magnetization is no longer conserved and the route to consensus is dramatically different than for the VM on degree-regular networks.

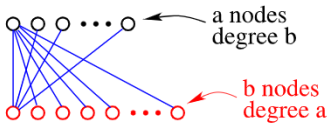

Fig. 4. The complete bipartite graph $K_{a,b}$.

A useful way to begin to understand the role of degree heterogeneity on VM dynamics is to study the simplest graph with different degrees, namely, the complete bipartite graph $K_{a,b}$ [46]. This graph consists of two subgroups, in which each member of subgroup a is connected to every member of subgroup b and vice versa. Thus $K_{a,b}$ consists of a nodes of degree b and b nodes of degree a (Fig. 4). On this network, it is a simple exercise to solve the VM dynamics. Let $N_{a,b}$ be the respective number of ↑ voters on each subgraph. In an update event, these numbers change according to

$$\begin{aligned}\mathrm{d}N_a &= \frac{a}{a+b}\left[\frac{a-N_a}{a}\frac{N_b}{b} - \frac{N_a}{a}\frac{b-N_b}{b}\right] \\ \mathrm{d}N_b &= \frac{b}{a+b}\left[\frac{b-N_b}{b}\frac{N_a}{a} - \frac{N_b}{b}\frac{a-N_a}{a}\right]\end{aligned} \tag{9}$$

Please cite this article in press as: S. Redner, Reality-inspired voter models: A mini-review, C. R. Physique (2019), https://doi.org/10.1016/j.crhy.2019.05.004

The gain term in dN_a accounts for flipping a $\downarrow$ voter in subgraph a due to its interaction with a $\uparrow$ voter in b, while the loss term accounts for flipping a $\uparrow$ voter in a. Since the time increment for an event $\delta t = 1/(a+b) = 1/N$, the subgraph densities $\rho_a = N_a/a$ and $\rho_b = N_b/b$ obey $\dot{\rho}_{a,b} = \rho_{b,a} - \rho_{a,b}$, with solution

$$\rho_{a,b}(t) = \tfrac{1}{2}[\rho_{a,b}(0) - \rho_{b,a}(0)]\, e^{-2t} + \tfrac{1}{2}[\rho_a(0) + \rho_b(0)] \tag{10}$$

Thus $\rho_a + \rho_b$ is asymptotically conserved and approaches the limiting value $\rho_\infty \equiv \frac{1}{2}[\rho_a(0) + \rho_b(0)]$, but the magnetization $m = (a\rho_a + b\rho_b)/(a+b)$ is not conserved [43]. Because $\rho_a + \rho_b$ is the conserved quantity, the sum of the subgraph densities in the final state equals 2 with probability $E(\rho_a, \rho_b)$, which is the exit probability to the state where all voters are in the $\uparrow$ state. Conservation therefore gives

$$E(\rho_a, \rho_b) = \tfrac{1}{2}[\rho_a(0) + \rho_b(0)] \tag{11}$$

When the voters on the two subgraphs are initially oppositely oriented, there is an equal probability of ending with all $\uparrow$ voters or all $\downarrow$ voters, *independent* of the subgraph sizes. In the extreme case of the star graph $K_{a,1}$, with $a \gg 1$ voters with $\uparrow$ opinion at the periphery and a single $\downarrow$ voter at the center, there is a 50% chance of $\downarrow$ consensus.

We follow the approach outlined in Sec. 2 to determine the consensus time $T(\rho_a, \rho_b)$. This time satisfies the backward Kolmogorov equation [25–27,46],

$$\begin{aligned} T(\rho_a, \rho_b) = {} & w(\rho_a, \rho_b \to \rho_a \pm \tfrac{1}{a}, \rho_b)[T(\rho_a \pm \tfrac{1}{a}, \rho_b) + \delta t] \\ & + w(\rho_a, \rho_b \to \rho_a, \rho_b \pm \tfrac{1}{b})[T(\rho_a, \rho_b \pm \tfrac{1}{b}) + \delta t] \\ & + w(\rho_a, \rho_b \to \rho_a, \rho_b)[T(\rho_a, \rho_b) + \delta t] \end{aligned} \tag{12}$$

which generalizes Eq. (4b) to the complete bipartite graph. The first term (which is actually a shorthand for the two contributions with a + sign and a − sign) accounts for flipping a $\downarrow$ ($\uparrow$) voter in subgraph a so that $\rho_a \to \rho_a \pm \frac{1}{a}$. The probability for flipping a $\downarrow$ voter in subgraph a is $w(\rho_a, \rho_b \to \rho_a + \frac{1}{a}, \rho_b) = \frac{a}{a+b}(1-\rho_a)\rho_b$, where $\frac{a}{a+b}(1-\rho_a)$ is the probability to choose a $\downarrow$ voter in subgraph a. Similar explanations apply for the other terms in Eq. (12). This equation is subject to the boundary conditions $T(0,0) = T(1,1) = 0$.

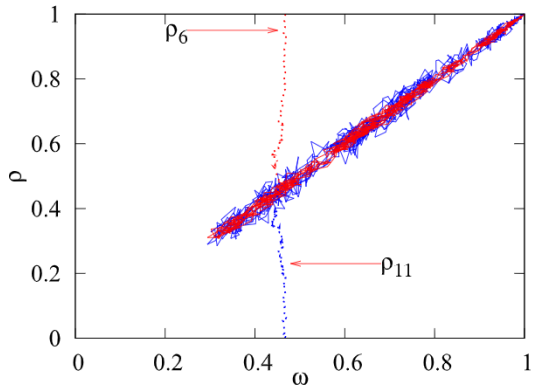

Fig. 5. Trajectories of $\rho_6(t)$ (degree less than $\mu_1 = 8$) and $\rho_{11}(t)$ (degree greater than μ_1) versus ω, for one realization of the voter model on a configuration model network of 2×10^5 nodes, with degree distribution $n_k \sim k^{-2.5}$, and average degree $\mu_1 = 8$. The initial state is $(\rho_{k>\mu_1}, \rho_{k\le\mu_1}) = (0, 1)$. The dotted curves show the initial transient for $t \lesssim 1$, after which diffusive motion leads to consensus at $(1, 1)$.

Expanding this recursion to second order, gives, after straightforward algebra,

$$N\delta t = (\rho_a - \rho_b)(\partial_a - \partial_b)T(\rho_a, \rho_b) - \tfrac{1}{2}(\rho_a + \rho_b - 2\rho_a\rho_b)\left(\tfrac{1}{a}\,\partial_a^2 + \tfrac{1}{b}\,\partial_b^2\right)T(\rho_a, \rho_b) \tag{13}$$

where ∂_i denotes partial derivative with respect to ρ_i. The first term on the right corresponds to a convection that drives the population to equal subgraph magnetizations in a time scale of order one, while the second term corresponds to the subsequent diffusive fluctuations that govern the ultimate approach to consensus (Fig. 5). We thus determine the consensus time by replacing the subgraph densities ρ_a and ρ_b by their common value ρ. Doing so ignores early-time transients when the subgraph densities are unequal. We also transform the derivatives with respect to ρ_a and ρ_b in Eq. (13) to derivative with respect to ρ to yield

$$\tfrac{1}{4}\,\rho(1-\rho)\left(\tfrac{1}{a} + \tfrac{1}{b}\right)\partial^2 T = -1 \tag{14a}$$

with solution

Please cite this article in press as: S. Redner, Reality-inspired voter models: A mini-review, C. R. Physique (2019), https://doi.org/10.1016/j.crhy.2019.05.004

$$T_N(\rho) = -\frac{4ab}{a+b}\,[(1-\rho)\ln(1-\rho) + \rho\ln\rho\,] \tag{14b}$$

Notice the close correspondence between the results given in Eqs. (14) with Eq. (5) and its defining differential equation. For $a = \mathcal{O}(1)$ and $b = \mathcal{O}(N)$ (star graph), the consensus time $T_N \sim \mathcal{O}(1)$, while if both a and b are $\mathcal{O}(N)$, then $T_N \sim \mathcal{O}(N)$, as on a complete graph.

This approach can be extended in a natural way to networks with an arbitrary distribution of degrees. If we neglect correlations between the degrees of neighboring nodes, then Eq. (12) readily generalizes from two densities on nodes of degrees a and b to an unlimited number of densities ρ_k on the set of nodes of any degree k. Now taking the continuum limit of this equation and making use of the conservation law that the degree-weighted density of ↑ voters [46]

$$\omega \equiv \sum_k k n_k \rho_k \Big/ \sum_k k n_k$$

is conserved, we eventually arrive at the counterpart of Eq. (14a), namely,

$$\frac{1}{N\mu_1^2}\sum_k k^2 n_k\,\omega(1-\omega)\;\partial_\omega^2 T = -1 \tag{15}$$

with $\mu_m = \sum_k k^m n_k$ the mth moment of the degree distribution. The solution for the consensus time is (compare again with Eq. (5))

$$\begin{aligned} T(\omega) &= -N\frac{\mu_1^2}{\mu_2}\,[(1-\omega)\ln(1-\omega) + \omega\ln\omega\,] \\ &\equiv N_{\rm eff}[(1-\omega)\ln(1-\omega) + \omega\ln\omega \end{aligned} \tag{16}$$

with $N_{\rm eff}$ the *effective* population size.

For a scale-free network whose degree distribution is given by $n_k \sim k^{-\nu}$, the mth moment of this distribution is given by

$$\mu_m \sim \int^{k_{\rm max}} k^m n_k\,{\rm d}k$$

Here $k_{\rm max} \sim N^{1/(\nu-1)}$ is the maximal degree in a finite network of N nodes, which obtained from the extremal condition $\int_{k_{\rm max}} k^{-\nu}\,{\rm d}k = N^{-1}$ [34]. Notice that the second moment diverges at the upper limit for $\nu \le 3$ while the first moment diverges for $\nu \le 2$. Assembling these results for the moments, the mean consensus time on a scale-free graph has the N dependence

$$T_N \sim \begin{cases} N & \nu > 3 \\ N/\ln N & \nu = 3 \\ N^{(2\nu-4)/(\nu-1)} & 2 < \nu < 3 \\ (\ln N)^2 & \nu = 2 \\ \mathcal{O}(1) & \nu < 2 \end{cases} \tag{17}$$

The primary result is that consensus is achieved quickly on networks with broad degree distributions. This rapid consensus is facilitated by "hubs"—nodes of the largest degrees that influence their very many neighbors. Moreover, there is a two time-scale route to consensus, with a rapid approach to a state where the densities of ↑ voters on nodes of any degree reach a common value (Fig. 5), after which diffusive fluctuations drive the approach to consensus.

5. Non-conserved dynamics

5.1. Majority rule

While the VM update rule is simple and natural, there are other plausible ways in which a group of voters might change opinions. A basic example is *majority rule*, for which there exists a vast social science literature (see e.g., [50–53]). From the mathematical perspective, there are two natural implementations of majority rule. One is that a voter adopts the state of the majority in its local neighborhood. This is just the update rule of the kinetic Ising model with single spin-flip dynamics at zero temperature [23,24]. This well-studied dynamics leads to a coarsening mosaic of ↑ and ↓ domains that usually, but not always (see e.g., [54,55]), ends in consensus.

Alternatively, a group of voters is selected and *all* voters in this group adopt the local majority opinion. Related models have been studied in various contexts [56–59]. Here we treat the situation where each voter has two opinion states and the group size equals three—the smallest possible size of a group with an odd number of neighbors. In an update, a group of three voters is selected at random from a total population of N, corresponding to the complete-graph or mean-field limit.

Please cite this article in press as: S. Redner, Reality-inspired voter models: A mini-review, C. R. Physique (2019), https://doi.org/10.1016/j.crhy.2019.05.004

These voters all adopt the group majority opinion and return to the general population [60]. This update is repeated until a finite population necessarily reaches consensus.

Let us first determine E_n, the exit probability that the population ends with all $\uparrow$ voters when starting with n $\uparrow$ voters. To compute E_n, note first that the quantity

$$\binom{3}{j}\binom{N-3}{n-j}\Big/\binom{N}{n}$$

is probability that a randomly chosen group of three voters has j voters of $\uparrow$ opinion and $3-j$ voters of $\downarrow$ opinion when an N-voter population contains n $\uparrow$ voters. This group becomes all $\uparrow$ for $j=2$, becomes all $\downarrow$ for $j=1$, while for $j=0$ or 3 there is no evolution. Thus E_n obeys the backward Kolmogorov equation

$$E_n = \left\{3\binom{N-3}{n-2}E_{n+1} + 3\binom{N-3}{n-1}E_{n-1} + \left[\binom{N-3}{n-3} + \binom{N-3}{n}\right]E_n\right\}\Big/\binom{N}{n} \tag{18a}$$

or

$$(n-1)(E_{n+1}-E_n) = (N-n-1)(E_n - E_{n-1}) \tag{18b}$$

This second-order recursion can be solved by standard methods [61], and the final result is

$$E_n = \sum_{j=1}^{n-1} \frac{\Gamma(N-2)}{\Gamma(j)\,\Gamma(N-j-1)} \tag{19a}$$

where $\Gamma(\cdot)$ is the Euler gamma function. Correspondingly, the probability to end with all $\downarrow$ voters is E_{N-n}. In the continuum limit, this result for E_n simplifies to

$$E_n \longrightarrow E(y) \simeq \tfrac{1}{2}\left[1+\mathrm{erf}(y/\sqrt{2})\right] \tag{19b}$$

with $y=(2n-N)/\sqrt{N}$. The curve of $E(y)$ versus y is a sigmoidal function that steepens as N increases and becomes a step function in the $N\to\infty$ limit. It becomes extremely unlikely that the initial minority wins in a large finite population.

Following the same reasoning as above, we also compute the consensus time, $T(n)$, when starting with n $\uparrow$ voters. This quantity obeys the recursion

$$T_n = \left\{3\binom{N-3}{n-2}(T_{n+1}+\delta T) + 3\binom{N-3}{n-1}(T_{n-1}+\delta T) + \left[\binom{N-3}{n-3} + \binom{N-3}{n}\right](T_n+\delta T)\right\}\Big/\binom{N}{n} \tag{20}$$

subject to the boundary conditions $T(0)=T(N)=0$. The natural choice for the time increment of an elemental update is $\delta T = 3/N$, so that each spin is updated once per unit time, on average. This inhomogeneous second-order recursion can again be solved by standard methods and the final result is (Fig. 6)

$$T_n = 1 + 2k(2k-1)\sum_{j=1}^{n-1}\frac{V_j}{\Gamma(j)\,\Gamma(2k-j)} \tag{21}$$

with

$$V_j = \sum_{i=1}^{k-j}\frac{\Gamma(k-i)\,\Gamma(k+i-1)}{(k-i+1)\,(k+i)}$$

where $k=\frac{1}{2}(N-1)$. While the exact expression is unwieldy, the $N\to\infty$ behavior of T_n is simple:

$$T(n) \simeq \begin{cases} 2\ln N & n = N/2 \\ \ln N & n \neq N/2 \end{cases} \tag{22}$$

On finite-dimensional lattices, surprisingly rich behavior arises that is distinct from both the VM and the zero-temperature kinetic Ising model. In one dimension, a natural update rule is: select a group of three contiguous spins that all adopt the majority opinion and repeat this step until consensus is reached. At long times, this rule leads to Ising-like dynamics in which the density of domain walls—the boundary between neighboring opposite-opinion voters—decays with time as $t^{-1/2}$.

On hypercubic d-dimensional lattices, a natural group definition is the von Neumann neighborhood—a voter and its $2d$ nearest neighbors. In an update, voters in a randomly selected neighborhood all adopt the majority opinion, and this update is repeated until consensus is reached. This leads to a dynamics that resembles the kinetic Ising model in that domain interfaces have non-zero surface tension. However, straight interfaces, which are stable in the kinetic Ising model and

Please cite this article in press as: S. Redner, Reality-inspired voter models: A mini-review, C. R. Physique (2019), https://doi.org/10.1016/j.crhy.2019.05.004

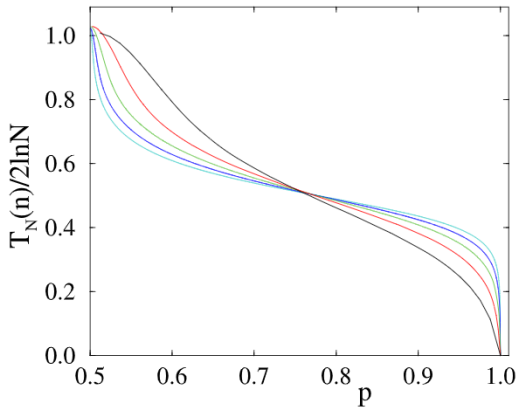

Fig. 6. Consensus time T_n versus $p = n/N$ for $N = 81$, 401, 2001, 10001, and 50001 (more step-like curves for larger N).

prevent the ground state from being reached, are unstable in majority rule. Thus consensus is always achieved in majority rule. Simulations indicate that the consensus time grows as N^ν, with the exponent ν continuously decreasing in the spatial dimension, with numerical values 2, 1.24, 0.72, and 0.56 for spatial dimension $d = 1, 2, 3$, and 4, respectively [62]. There is currently no analytical understanding of this unusual dimension dependence of the consensus time.

5.2. Nonlinear update rules

There are many socially plausible update rules in which the flip rate of a voter depends nonlinearly on the fraction of disagreeing neighbors. We discuss two such examples: (i) the *vacillating* voter model (VVM) [63] and (ii) the *non-conserved* voter model (NVM) [64,65].

In a VVM update, a voter consults two of its neighbors and changes opinion if it disagrees with either of them. This irresolution causes a global bias toward zero magnetization. Concretely, the VVM update rules are as follows.

1. A random voter i picks a random neighbor j. If j disagrees with i, then i changes state.
2. If j and i agree, then i picks another random neighbor k and adopts its state.
3. Repeat steps 1–2 until consensus is reached.

It is easily checked that the flip probability for a vacillating voter on the square lattice equals 0, $\frac{1}{2}$, $\frac{5}{6}$, and 1, respectively, when the number of misaligned neighbors is 0, 1, 2, and ≥ 3. In contrast, for the VM, the flip probability is $\frac{k}{4}$, where k is the number of disagreeing neighbors.

In the mean-field limit, the density x of $\uparrow$ voters evolves by the rate equation

$$\begin{aligned}\dot{x} &= -x\left[1-x^2\right] + (1-x)\left[1-(1-x)^2\right] \\ &= x(1-x)(1-2x)\end{aligned} \tag{23}$$

The first term on the right accounts for the loss of $\uparrow$ voters in which a $\uparrow$ voter is first picked (the factor x), and then the neighborhood cannot consist of two $\uparrow$ voters (the factor $1-x^2$). Similarly, in the second (gain) term, a $\downarrow$ voter is first picked, and then the neighborhood must contain at least one $\uparrow$ voter. From this rate equation, there are unstable fixed points at $x = 0, 1$ and a stable fixed point at $x = 1/2$. Thus the population is driven to the zero-magnetization state.

Because consensus is the only absorbing state of the stochastic dynamics, a finite population ultimately reaches this state. To characterize the approach to consensus, we determine the exit probability $E(n)$, the probability that a population with n $\uparrow$ voters of out N voters reaches $\uparrow$ consensus. This exit probability obeys a backward equation of the form given in Eq. (4a), with transition probabilities that are, in the continuum limit,

$$\begin{aligned} w_{n\to n+1} &= (1-x)\left[1-(1-x)^2\right] \\ w_{n\to n-1} &= x(1-x^2) \\ w_{n\to n} &= x^3 + (1-x)^3 \end{aligned}$$

Substituting these probabilities in the backward equation and taking the continuum limit, gives

$$\frac{3x(1-x)}{2N}\frac{\partial^2 E}{\partial x^2} + x(1-x)(1-2x)\frac{\partial E}{\partial x} = 0 \tag{24}$$

Please cite this article in press as: S. Redner, Reality-inspired voter models: A mini-review, C. R. Physique (2019), https://doi.org/10.1016/j.crhy.2019.05.004

with solution

$$E(x) = \int_{-1/2}^{x-1/2} e^{2Ny^2/3}\, dy \Big/ \int_{-1/2}^{1/2} e^{2Ny^2/3}\, dy \tag{25}$$

The exit probability approaches an anti-sigmoidal shape in which $E(x)$ attains the nearly constant value 1/2 over a progressively wider range for increasing N (Fig. 7). This behavior reflects the voting bias towards zero magnetization. Thus a population with an arbitrary initial magnetization is driven to an effective potential well at $x = \frac{1}{2}$ (equivalently at $m = 0$), and consensus is achieved by the population surmounting this effective potential barrier. As a result, the exit probability becomes nearly independent of x for large N.

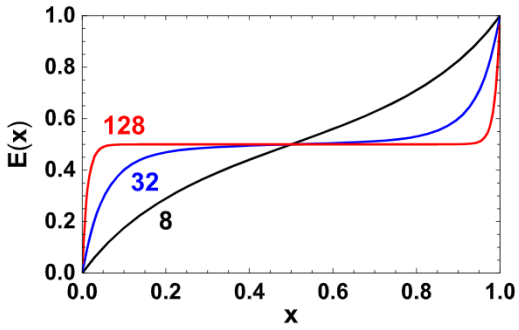

Fig. 7. Exit probability $E(x)$ versus the density of ↑ voters x for the cases $N = 8$, 32, and 128.

In the same spirit, the consensus time obeys (24) but with the right-hand side now equal to -1. The formal solution is elementary but ugly, and is not expressible in closed form. The main result, however, is that the consensus time scales exponentially in N. Again, in contrast to the VM, the global bias drives the population into an effective potential well that must be surmounted to reach consensus, leading to a large consensus time.

In the NVM, the flip rate of a voter explicitly depends nonlinearly on the fraction of disagreeing neighbors. We treat the simplest setting of one dimension. Let r_f denote the flip rate of a voter when the fraction of disagreeing neighbors is f (Fig. 8). It is natural to impose $r_0 = 0$, so that no evolution occurs when there is local consensus. Then the most general description involves two parameters, r_1 and r_2. By absorbing one rate into the overall time scale, the only parameter is the ratio $\gamma = r_2/r_1$. For $\gamma > 2$, the influence of two neighbors is more than twice that of one neighbor. For $\gamma \to \infty$, a voter changes opinion by "unanimity rule"—all neighbors must have the opposite opinion [66]. The case $\gamma = 2$ corresponds to the classical voter model. For $\gamma < 2$, one disagreeing neighbor is more effective in triggering an opinion change than in the classical voter model, and the limiting case $\gamma = 1$ corresponds to the vacillating voter model (VVM).

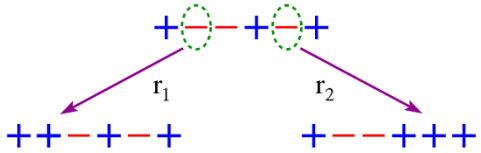

Fig. 8. Update events in the non-conserved voter model in one dimension. A voter changes state with rate r_1 if it has 1 disagreeing neighbor (left), and with rate r_2 if it has 2 disagreeing neighbors (right).

It is a pleasant game to work out the NVM flip rate in one dimension. For a voter at site i, this rate is

$$w_i = \gamma + 2 - \gamma\sigma_i(\sigma_{i-1} + \gamma\sigma_{i+1}) + (\gamma - 2)\sigma_{i-1}\sigma_{i+1} \tag{26}$$

Left/right symmetry mandates that the $\sigma_i\sigma_{i+1}$ and the $\sigma_i\sigma_{i-1}$ terms have the same coefficient. For $\gamma = 2$, the $\sigma_{i-1}\sigma_{i+1}$ term vanishes, and the VM equation of motion is recovered. We shall see, however, that the $\sigma_{i-1}\sigma_{i+1}$ term couples the rate equation for the single-body quantity σ_i to 3-body terms (see also Ref. [67]).

Because of this coupling, it is not possible to solve the NVM model exactly. Nevertheless, we obtain an approximate solution by truncating the hierarchy of rate equations for higher-order correlation functions. Using (2), the time dependence of the mean opinion $s_i \equiv \langle\sigma_i\rangle$ is given by

$$\dot{s}_i = 2\gamma(s_{i+1} + s_{i-1}) - 2(\gamma + 2)s_i - 2(\gamma - 2)\langle\sigma_{i-1}\sigma_i\sigma_{i+1}\rangle \tag{27}$$

Please cite this article in press as: S. Redner, Reality-inspired voter models: A mini-review, C. R. Physique (2019), https://doi.org/10.1016/j.crhy.2019.05.004

For $\gamma = 2$, the nonlinear term vanishes and the resulting diffusion-like equation is exactly soluble. However, for $\gamma \neq 2$, the equation for s_i is coupled to higher-order correlations.

Let us first neglect all correlations and assume that $\langle \sigma_{j-1}\sigma_j\sigma_{j+1}\rangle \approx m^3$, with the magnetization $m = \langle s_i\rangle$. With this assumption, Eq. (27) reduces to

$$\dot{m} = 2(\gamma - 2)(m - m^3) \tag{28}$$

so that the magnetization is not conserved for $\gamma \neq 2$. The stable solutions of Eq. (28) are either consensus ($m = \pm 1$) when $\gamma > 2$, or stasis, with equal densities of the two types of voters ($m = 0$), when $\gamma < 2$.

A better assumption is to truncate the hierarchy of equations for multi-spin correlation functions at higher order [63,68]. Consider the rate equation for the nearest-neighbor correlation function $\langle \sigma_j\sigma_{j+1}\rangle$:

$$\frac{\partial\langle \sigma_j\sigma_{j+1}\rangle}{\partial t} = -2(\gamma - 2)\left[\langle \sigma_{j-1}\sigma_j\rangle + \langle \sigma_{j+1}\sigma_{j+2}\rangle\right] + 2\gamma\left[\langle \sigma_{j-1}\sigma_{j+1}\rangle + \langle \sigma_j\sigma_{j+2}\rangle\right] + 4\gamma - 4(\gamma + 2)\langle \sigma_j\sigma_{j+1}\rangle \tag{29}$$

To close this equation, we need to approximate the second-neighbor correlation functions $\langle \sigma_j\sigma_{j+2}\rangle$. To make progress, let us first examine the role of domain walls—nearest-neighbor anti-aligned voters—whose density is $\rho = (1 - \langle \sigma_i\sigma_{i+1}\rangle)/2$, on the dynamics. According to the transition rate (26), an isolated domain wall diffuses freely for any γ. However, when two domain walls are adjacent, they annihilate with probability $P_a = \gamma/(2 + \gamma)$ or they hop away from each other with probability $P_h = 2/(2 + \gamma)$. Thus when $\gamma > 2$, $P_a > P_h$, and adjacent domain walls tend to annihilate, while they repel when $\gamma < 2$. The interaction of two domain walls is therefore equivalent to single-species annihilation, $A + A \to 0$, but with a reaction rate that is modified compared to freely diffusing particles because of this interaction. Nevertheless, the domain wall density asymptotically decays as $t^{-1/2}$ for any $\gamma < \infty$, but with an interaction-independent amplitude [69].

Since domain walls become widely separated at long times, we therefore approximate the second-neighbor correlation function as $\langle \sigma_j\sigma_{j+2}\rangle \approx \langle \sigma_j\sigma_{j+1}\rangle$ [63]. We also write the nearest-neighbor correlation function $\langle \sigma_j\sigma_{j+1}\rangle$ for a spatially homogeneous population as m_2 for notational simplicity. Now the rate equation (29) for m_2 becomes

$$\dot{m}_2 = 4\gamma - 4\gamma m_2 \tag{30}$$

For the uncorrelated initial condition, $m_2(0) = m(0)^2$, the solution is

$$m_2(t) = 1 + \left[m(0)^2 - 1\right] e^{-4\gamma t} \tag{31}$$

where $m(0) \equiv \langle s_j(0)\rangle$ is the magnetization at $t = 0$.

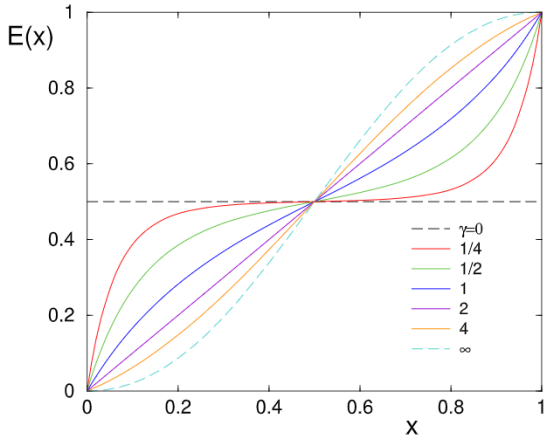

Fig. 9. Exit probability $E(x)$ for the non-conserved voter model in one dimension from Eq. (34) as a function of the initial density of ↑ voters x for different values of γ.

In a similar spirit, we decouple the 3-spin correlation function as $\langle \sigma_{j-1}\sigma_j\sigma_{j+1}\rangle \approx m m_2$ [63] and average over all sites to simplify the rate equation (27) for the mean spin in a spatially homogeneous population to

$$\dot{m} = 2(2 - \gamma)m\, e^{-4\gamma t}[m(0)^2 - 1] \tag{32}$$

Solving this equation and taking the $t \to \infty$ limit, we obtain a non-trivial relation between the final and initial magnetizations:

$$m(\infty) = m(0)\, e^{(2-\gamma)(m(0)^2-1)/2\gamma} \tag{33}$$

Please cite this article in press as: S. Redner, Reality-inspired voter models: A mini-review, C. R. Physique (2019), https://doi.org/10.1016/j.crhy.2019.05.004

However, the average magnetization in a finite population does not perpetually fluctuate around this asymptotic value but ultimately reaches ± 1 because consensus is the only absorbing state of the stochastic dynamics. We characterize this consensus by the exit probability $E(x)$ to reach $\uparrow$ consensus when initially $n = xN$ out of N voters are in the $\uparrow$ state. Since the density of $\uparrow$ voters $x = (1+m)/2$, and $m(\infty) = 2E(x) - 1$ (see (3)), Eq. (33) gives (Fig. 9)

$$E(x) = \frac{1}{2}\left[(2x-1)\, e^{2x(2-\gamma)(x-1)/\gamma} + 1\right] \tag{34}$$

The non-linear behavior of $E(x)$ versus x given Fig. 9 arises generally in opinion evolution models where the average magnetization is not conserved, such as the majority rule model of Sec. 5.1. These sigmoidal (initial slope greater than 1) and anti-sigmoidal curves are generic behaviors for the exit probability. Because of the generality of these two classes, they have been widely investigated in the social science literature, where a variety of mechanisms have been proposed to generate these two basic forms for the exit probability [70,71].

6. More than two states

6.1. Constrained 3-choice voting

There is nothing sacrosanct about two voting states. A natural extension of the VM is to allow a voter to have any number voting states. For k voting states and a VM update rule (Sec. 2), the resulting dynamics is again VM like. If we label the states as $\{a, b, c, \ldots, k\}$ and collectively denote the voter states $\{b, c, \ldots, k\}$ as $\bar{a}$, then the dynamics of a and $\bar{a}$ is just the usual 2-state voter model, with the initial density of $\bar{a}$ equal to the sum of the initial densities of $\{b, c, \ldots, k\}$.

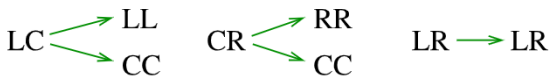

Fig. 10. Update events for different pair states in constrained 3-choice voting.

More interesting behavior arises if the interactions between the states are not all identical. A simple extension of this genre is the *constrained 3-state voter model* [72] (Fig. 10), where we suggestively label the states as leftists L (with density x), rightists R (density y), and centrists C (density $z = 1 - x - y$). In an elemental interaction, the pair LC equiprobably transforms to LL or CC, while CR equiprobably transforms to RR or CC. That is, there is usual voter model dynamics between a centrist and a voter in any other opinion state. However leftists and rightists are sufficiently separated in opinion space that do not interact.

In this 3-choice model, updates between interacting pairs occur repeatedly until the population can no longer evolve. While the sense of the interactions are either neutral or consensus promoting, the population can get trapped in a frozen state that consists of only leftists or of only rightists. This freezing, even though the elemental update is consensus promoting, also occurs in the venerable Axelrod model [73–75] that will be discussed below.

We now outline how to determine the probability $F(x, y)$ that the population reaches a frozen state as a function of the initial densities, x and y. This quantity is just the first-passage probability for a trajectory to hit the line $x + y = 1$ when it starts at some point within the tetrahedral region $x + y + z < 1$ in the composition space spanned by the densities x, y, and z (Fig. 11). We need to impose the boundary conditions $F = 0$ for $x = 0$ and $y = 0$, where the probability of reaching the frozen state is zero, and $F = 1$ on the line segment $x + y = 1$. This first-passage probability obeys the backward Kolmogorov equation (see the discussion that explained Eq. (4a))

$$F(x, y) = p_x[F(x-\delta, y) + F(x+\delta, y)] + p_y[F(x, y-\delta) + F(x, y+\delta)] + [1 - 2(p_x + p_y)]F(x, y) \tag{35}$$

where

$$p_x = N_- N_0/[N(N-1)]$$
$$p_y = N_+ N_0/[N(N-1)]$$

are the transition probabilities for $(N_-, N_0) \to (N_- \pm 1, N_0 \mp 1)$ and $(N_+, N_0) \to (N_+ \pm 1, N_0 \mp 1)$, respectively, and $\delta = 1/N$.

In the continuum limit, (35) reduces to

$$x\frac{\partial^2 F(x, y)}{\partial x^2} + y\frac{\partial^2 F(x, y)}{\partial y^2} = 0 \tag{36}$$

subject to the mixed boundary conditions $F(x, 0) = F(0, y) = 0$, $F(x, 1-x) = 1$. This mixed boundary condition is the feature that makes it difficult to obtain a direct analytical solution. However, after a series of coordinate transformations, Eq. (36) can be mapped onto a Schrödinger equation in the presence of a specific potential well, which is soluble [72]. By these means, the solution to Eq. (36) is [72]

Please cite this article in press as: S. Redner, Reality-inspired voter models: A mini-review, C. R. Physique (2019), https://doi.org/10.1016/j.crhy.2019.05.004

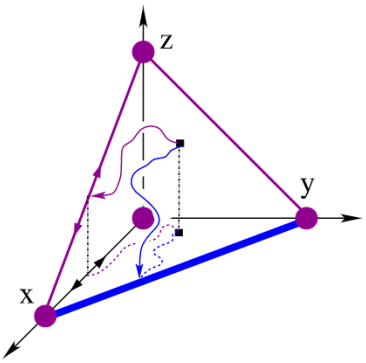

Fig. 11. The composition triangle $x + y + z = 1$. The purple dots denote consensus states and the heavy blue line denotes frozen final states where no centrists remain. Typical trajectories are shown. When a trajectory reaches the lines $x = 0$ or $y = 0$, the trajectory subsequently remains on this line until consensus is necessarily reached.

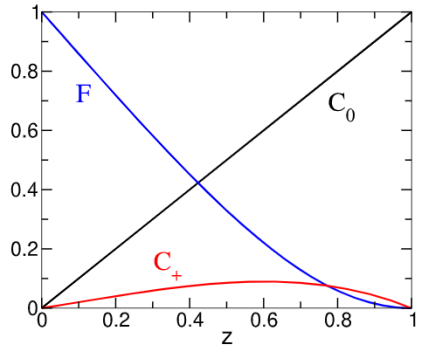

Fig. 12. The probabilities to reach the frozen state, F, and to reach the centrist and extremist consensus states, C_0 and C_+, respectively, as a function of the initial density of centrists z for the case of equal initial densities of leftists and rightists, $y/x = 1$.

$$F(x, y) = \sum_{n \text{ odd}} \frac{2(2n+1)}{n(n+1)} \sqrt{xy}\,(x+y)^n\, P_n^1\left(\frac{x-y}{x+y}\right) \tag{37}$$

where P_n^1 is the associated Legendre function. By a similarly tedious calculation, the probability to reach $\downarrow$ consensus as a function of the initial densities x and y is

$$C_-(x, y) = x - \sum_{n=1}^{\infty} \frac{(2n+1)}{n(n+1)} \sqrt{xy}\,(x+y)^n\, P_n^1\left(\frac{x-y}{x+y}\right) \tag{38}$$

The probability to reach $\uparrow$ consensus, $C_+(x, y)$, is obtained by the obvious symmetry $C_+(x, y) = C_-(y, x)$.

One of the main features of the final-state probabilities in Fig. 12 is that centrists are needed to catalyze consensus. As the centrist density $z \to 1$, the probability of reaching a frozen state goes to zero. Another comforting feature of this figure is that extremist consensus is relatively unlikely to occur.

6.2. Axelrod model

Some societies culturally fragment, even though individuals may try to reach agreement with acquaintances. The Axelrod model provides a simple description for this dichotomy [73–75]. Here, each individual possesses F characteristic features—for example, preferences for sports, for music, for food, *etc*—that each can assume q distinct values. In an update, a pair of agents is selected at random. If the agents disagree on all features, no interaction occurs. However, if the agents agree on at least one feature, they interact with probability equal to the fraction of shared features. In an interaction, a previously unshared feature is selected at random and one agent copies the preference for this feature from its interaction partner. While the interaction ostensibly brings agents closer together, the restriction that only sufficiently compatible individuals interact can prevent the population from reaching consensus.

Depending on the parameters (F, q), the Axelrod model on a finite-dimensional lattice undergoes a phase transition between consensus and a frozen discordant state, where each interacting pair is incompatible [73–79]. In the mean-field limit, the corresponding transition is between a steady state with perpetual social "churn" and a frozen state. There is also

Please cite this article in press as: S. Redner, Reality-inspired voter models: A mini-review, C. R. Physique (2019), https://doi.org/10.1016/j.crhy.2019.05.004

a non-monotonic time dependence of the societal activity level [76] that occurs over a very long time scale [76,80]. This long time scale is unexpected because the underlying dynamical equations (Eqs. (39) below) have rates of the order of one. Important examples where dynamics with rates of the order of 1 leads to anomalously long time scales include the Lorenz model [81], the three-species competition species models [82], and HIV [83]. In the Lorenz model, although the dynamics is a contracting map, trajectories can fall into a strange attractor with very long period dynamics. In HIV, after an individual contracts the disease, there is an immune response over several months, followed by a latency period that can last beyond a decade, during which an individual's T-cell level slowly diminishes. Our results for the Axelrod model provide some insight into how widely separated time scales can arise in a simple dynamical system.

To simplify the modeling as much as possible, we discuss a mean-field version in which each agent has a small and fixed number z of interaction partners, corresponding to a degree-regular random graph. We also restrict to the simplest non-trivial case of $F = 2$ features. Thus there are 3 types of links between individuals: links with no shared features (type 0), and links with both features shared (type 2). These two types of links are inactive because neither individual changes its state across such links. Finally, there are links of type 1 where a single feature is shared, which are the only active links in the population.

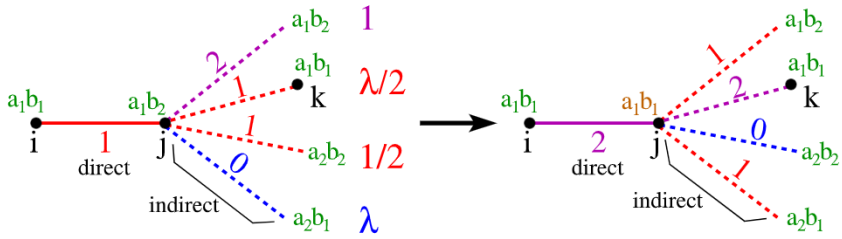

Fig. 13. State-changing indirect updates on links jk (dashed lines) when agent j changes state from $a_1b_2 \to a_1b_1$ (green to brown) in a direct interaction with agent i (solid line). The rates of each type of link-changing event are indicated. The number associated with each link indicates the number of shared features across the link. Links are also color coded by the number of shared features; magenta (2 shared features), red (1 shared feature and therefore active), and blue (no shared features).

By accounting for the various interaction events, the time dependence of the fraction of links of type i ($i = 0, 1, 2$) when a single agent changes its state is described by the rate equations [80]

$$\begin{aligned}
\dot{P}_0 &= \frac{z-1}{z} P_1 \left(-\lambda P_0 + \frac{1}{2} P_1 \right) \\
\dot{P}_1 &= -\frac{P_1}{z} + \frac{z-1}{z} P_1 \left(\lambda P_0 - \frac{1+\lambda}{2} P_1 + P_2 \right) \\
\dot{P}_2 &= \frac{P_1}{z} + \frac{z-1}{z} P_1 \left(\frac{\lambda}{2} P_1 - P_2 \right)
\end{aligned} \tag{39}$$

where z is the number of neighbors of each individual. The first term on the right-hand sides of the first two equations account for the direct interaction between agents i and j that changes a link of type 1 to type 2. For example, in $\dot{P}_1$, a type-1 link and the shared feature across this link is chosen with probability $P_1/2$ in an update event. This update decrements the number of type-1 links by one in a time $dt = 1/N$, where N is the population size. Assembling these factors gives the term $-P_1/z$ in this equation.

The remaining terms in the rate equations represent indirect interactions. For example, if agent j changes state from (a_1, b_2) to (a_1, b_1) then the link jk that joins to agent k in state (a_1, b_1) changes from type 1 to type 2 (Fig. 13). The probability for this event is proportional to $\lambda P_1/2$: P_1 is the probability that the indirect link is of type 1, the factor 1/2 accounts for the fact that only the first feature of agents j and k can be shared, while λ is the conditional probability that i and k share one feature that is simultaneously not shared with j.

If the distribution of preferences is uniform, then $\lambda = 1/(q-1)$. While λ generally depends on the densities P_m, the simulations presented in Ref. [80] indicate that λ is roughly constant and close to $1/(q-1)$. When we use this assumption, the rate equations (39) become soluble. The solution itself is too unwieldy to display here (the full solution is given in Ref. [80]), but the main result is quite striking (Fig. 14). The crucial feature is that there is a dramatic non-monotonicity in the density of active links, in which the time scale for the crossover between a nearly inactive state and an active steady state diverges as $q \to q_c = 2(z-1) + 2\sqrt{(z-1)(z-2)}$. While this strange behavior is the prediction from the mathematical solution to the rate equations (39), the physical mechanism that underlies this long-time non-monotonicity is not understood.

7. Compromise models

The bounded confidence, or compromise, model accounts for the human attribute that individuals often compromise their positions in an interaction. This class of appealing models was introduced in the physics literature in Refs. [84,85]. For

Please cite this article in press as: S. Redner, Reality-inspired voter models: A mini-review, C. R. Physique (2019), https://doi.org/10.1016/j.crhy.2019.05.004

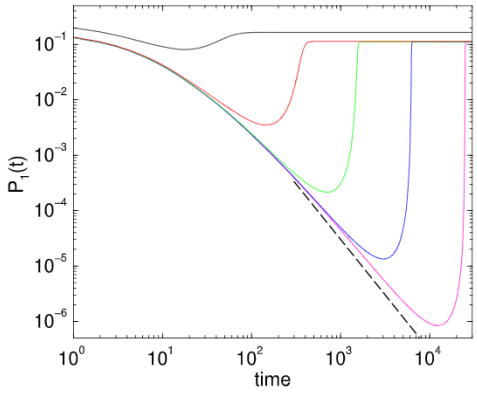

Fig. 14. Density of active links $P_1(t)$ for $q = q_c - 4^{-k}$, with $k = -1, 1, 3, 5$, and 7 (progressively lower minima). Each agent has $z = 4$ neighbors. The dashed curve shows how $P_1 \to 0$ for $q = q_c + 4^{-6}$.

simplicity, we take the opinion of individual i as a real coordinate x_i in a one-dimensional opinion space. The state of the population is updated as follows: Two agents are selected at random. If their opinions are separated by a distance less than a threshold that we take as fixed and equal to 1, they compromise; conversely, if their opinions are separated by a distance larger than 1, they do not interact (Fig. 15). This update step is repeated until the opinions of all individuals reach a static limit.

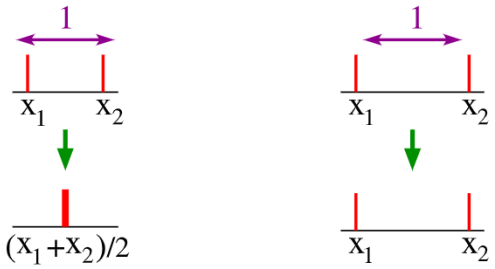

Fig. 15. Possible updates in the compromise model. Two agents with opinions x_1 and x_2 with $|x_2 - x_1| < 1$ compromise. Otherwise there is no opinion change.

Suppose that each agent is initially assigned an opinion x from the uniform distribution in $[-\Delta, \Delta]$, with Δ the only model parameter. According to the update rule given above, the opinions of a randomly selected pair of agents change according to (Fig. 15)

$$(x_1, x_2) \to \tfrac{1}{2}\,(x_1 + x_2, x_1 + x_2) \qquad |x_2 - x_1| < 1$$
$$(x_1, x_2) \to (x_1, x_2) \qquad |x_2 - x_1| > 1$$

A natural way to determine the time evolution of the distribution of opinions, $P(x,t)$, is to perform numerical simulations of the process defined above. However, such simulations become inefficient when agents opinions are close. In this case, it becomes necessary to update the opinions of agents many times for their opinions to change by a small amount.

It is much more efficient to numerically integrate the master equation that describes the time dependence of $P(x,t)$ because there is no "slowing down" of the dynamics. The master equation for the opinion distribution is

$$\frac{\partial}{\partial t} P(x,t) \iint\limits_{|x_1 - x_2| < 1} dx_1\, dx_2\, P(x_1,t) P(x_2,t) \times \left[\delta\left((x - \tfrac{1}{2}(x_1 + x_2)\right) - \delta(x - x_1)\right] \tag{40}$$

While this equation does not appear to be soluble, it can be integrated with high precision [86] in an efficient way, and the strikingly beautiful final state bifurcation diagram is shown in Fig. 16. For $\Delta < \Delta_1 = 1$, all pairs of individuals are compatible and the final state is consensus at $x = 0$. However, for $\Delta > \Delta_1$, a bifurcation arises in which a small fraction of extremists—both positive and negative—splits off from centrist consensus and forms a positive and a negative extremist group. As Δ increases still further, the extremists become progressively more extreme until a second bifurcation at $\Delta = \Delta_2 \approx 1.871$, where the centrist group splits into center-left and center-right groups, with nobody left in the center. At $\Delta = \Delta_3 \approx 2.248$, there is a third bifurcation where leftists and rightists have moved sufficiently far from the center that a new centrist group can nucleate.

Please cite this article in press as: S. Redner, Reality-inspired voter models: A mini-review, C. R. Physique (2019), https://doi.org/10.1016/j.crhy.2019.05.004

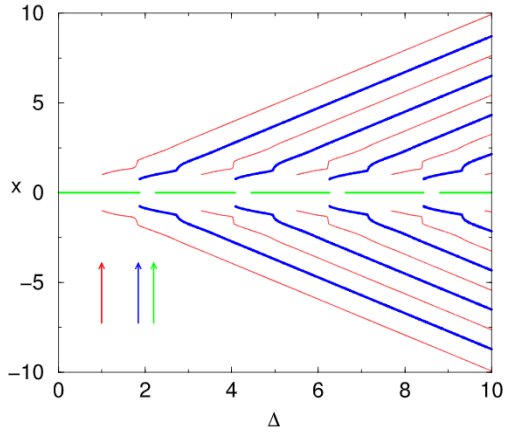

Fig. 16. The final opinion distribution as a function of the interaction threshold Δ. Vertical arrows mark the first 3 bifurcations at $\Delta_1 = 1$, $\Delta_2 \approx 1.871$ and $\Delta_3 \approx 2.248$.

As Δ continues to increase, this sequence of bifurcations systematically repeats. For fixed Δ, the spectrum of opinion states qualitatively mirrors what has happened in some multiparty parliamentary democracies. The important feature of the compromise model is that a too narrow compromise range leads to a fragmented polity, where each party lives within its own "echo chamber" and has no interaction with other parties.

8. Outlook

The venerable voter model has played a central role in probability theory and in statistical physics because it is one of the few exactly soluble many-particle interacting systems. The voter model has also been a starting point to describe a variety of social phenomena. However, the basic voter model is clearly too idealized to be of direct empirical relevance and much research has been devoted to incorporating socially motivated aspects of decision making into the model. In the absence of a correspondence between model parameters and empirical data, these generalizations should not be oversold as descriptions of social reality, but rather, as potentially useful descriptions of how opinions in a large population can change over time.

In this short review, a number of these extensions of the voter model were presented. These generalizations by no means cover the range of work of this genre, but we hope to have given the reader a useful perspective. In spite of their obvious shortcomings, each of the models presented here reveals rich phenomenology and appealing methodological aspects.

A basic message from these modeling efforts is that incorporating any realistic feature of decision making typically leads to either a dramatically hindered approach to consensus or to the prevention of consensus altogether. This prevention of consensus addresses one of the glaring unrealistic features of the voter model in that consensus is always achieved. Models such as those outlined here can also help to quantify verbal predictions that often appear in the social science literature and help determine which types of models could reproduce empirical observations. Thus from the optimistic perspective, perhaps some of these generalizations point the way to properly calibrated models of social dynamics.

I thank my collaborators who contributed substantially to the results presented here: Tibor Antal, Eli Ben-Naim, Pu Chen, Nathaniel Gibert, Paul Krapivsky, Renaud Lambiotte, Naoki Masuda, Vishal Sood, Federico Vazquez, and Dan Volovik. I am also grateful to Mirta Galesic for a critically reading of a draft of this manuscript and for many helpful suggestions. I also thank the NSF for financial support during the period of this research through grants DMR-0227670, DMR-0535503, DMR-0906504, as well as DOE grant W-7405-ENG-36 when the author spent a year at the Center for Nonlinear Studies at Los Alamos National Lab.

References

[1] P. Clifford, A. Sudbury, A model for spatial conflict, Biometrika 60 (1973) 581.
[2] R.A. Holley, T.M. Liggett, Ergodic theorems for weakly interacting infinite systems and the voter model, Ann. Probab. 3 (1975) 643.
[3] J.T. Cox, Coalescing random walks and voter model consensus times on the torus in $\mathbb{Z}$, Ann. Probab. 17 (1989) 1333.
[4] T.M. Liggett, Stochastic Interacting Systems: Contact, Voter, and Exclusion Processes, Springer, New York, 1999.
[5] P.L. Krapivsky, Kinetics of monomer-monomer surface catalytic reactions, Phys. Rev. A 45 (1992) 1067.
[6] L. Frachebourg, P.L. Krapivsky, Exact results for kinetics of catalytic reactions, Phys. Rev. E 53 (1996) R3009.
[7] I. Dornic, H. Chaté, J. Chave, H. Hinrichsen, Critical coarsening without surface tension: the universality class of the voter model, Phys. Rev. Lett. 87 (2001) 045701.
[8] C. Castellano, S. Fortunato, V. Loreto, Statistical physics of social dynamics, Rev. Mod. Phys. 81 (2009) 591.
[9] P.L. Krapivsky, S. Redner, E. Ben-Naim, A Kinetic View of Statistical Physics, Cambridge University Press, Cambridge, UK, 2010.
[10] A. Baronchelli, The emergence of consensus: a primer, R. Soc. Open Sci. 5 (2018) 172189.
[11] A. Jędrzejewski, K. Sznajd-Weron, Statistical physics of opinion formation: is it a SPOOF? C. R. Physique 20 (2019), https://doi.org/10.1016/j.crhy.2019.05.002, in this issue.

Please cite this article in press as: S. Redner, Reality-inspired voter models: A mini-review, C. R. Physique (2019), https://doi.org/10.1016/j.crhy.2019.05.004

[12] M. Faloutsos, P. Faloutsos, C. Faloutsos, On power-law relationships of the Internet topology, Comput. Commun. Rev. 29 (1999) 251.
[13] A. Broder, R. Kumar, F. Maghoul, P. Raghavan, S. Rajagopalan, R. Stata, A. Tomkins, J. Wiener, Graph structure in the Web, Comput. Netw. 33 (2000) 309.
[14] M.E.J. Newman, The structure of scientific collaboration networks, Proc. Natl. Acad. Sci. USA 98 (2001) 404.
[15] T. Gross, C.J.D. D'Lima, B. Blasius, Epidemic dynamics on an adaptive network, Phys. Rev. Lett. 96 (2006) 208701.
[16] P. Holme, M.E.J. Newman, Nonequilibrium phase transition in the coevolution of networks and opinions, Phys. Rev. E 74 (2006) 056108.
[17] B. Kozma, A. Barrat, Consensus formation on adaptive networks, Phys. Rev. E 77 (2008) 016102.
[18] L.B. Shaw, I.B. Schwartz, Fluctuating epidemics on adaptive networks, Phys. Rev. E 77 (2008) 066101.
[19] L.B. Shaw, I.B. Schwartz, Enhanced vaccine control of epidemics in adaptive networks, Phys. Rev. E 81 (2010) 046120.
[20] R. Durrett, J.P. Gleeson, A.L. Lloyd, P.J. Mucha, F. Shi, D. Sivakoff, J.E.S. Socolar, C. Varghese, Graph fission in an evolving voter model, Proc. Natl. Acad. Sci. USA 109 (2012) 3682.
[21] T.C. Rogers, T. Gross, Consensus time and conformity in the adaptive voter model, Phys. Rev. E 88 (2013) 030102.
[22] M. Galesic, D.L. Stein, Statistical physics models of belief dynamics: theory and empirical tests, Physica A 519 (2019) 275.
[23] J.D. Gunton, M. San Miguel, P.S. Sahni, in: C. Domb, J.L. Lebowitz (Eds.), Phase Transitions and Critical Phenomena, Vol. 8, Academic Press, New York, 1983.
[24] A.J. Bray, Theory of phase-ordering kinetics, Adv. Phys. 43 (1994) 357.
[25] A. Kolmogoroff, On analytical methods in probability theory, Math. Ann. 104 (1931) 415.
[26] N.G. van Kampen, Stochastic Processes in Physics and Chemistry, 2nd ed., North-Holland, Amsterdam, 1997.
[27] S. Redner, A Guide to First-Passage Processes, Cambridge University Press, New York, 2001.
[28] S.E. Asch, in: H. Guetzkow (Ed.), Groups, Leadership and Men, Carnegie Press, Pittsburgh, PA, 1951.
[29] R.L. Kendal, N.J. Boogert, L. Rendell, K.N. Laland, M. Webster, P.L. Jones, Social learning strategies: bridge-building between fields, Trends Cogn. Sci. 22 (2018) 651.
[30] N. Masuda, N. Gibert, S. Redner, Heterogeneous voter models, Phys. Rev. E 82 (2010) 010103.
[31] M. Granovetter, Threshold models of collective behavior, Am. J. Sociol. 83 (1978) 1420.
[32] D.J. Watts, A simple model of global cascades on random networks, Proc. Natl. Acad. Sci. USA 99 (2002) 5766.
[33] M.O. Jackson, Social and Economic Networks, Princeton University Press, Princeton, NJ, USA, 2008.
[34] J. Galambos, The Asymptotic Theory of Extreme Order Statistics, Krieger Publishing Co., Malabar, FL, 1987.
[35] S. Moscovici, Toward a theory of conversion behavior, Adv. Exp. Soc. Psychol. 13 (1980) 209.
[36] S. Moscovici, Innovation and minority influence, in: S. Moscovic, G. Mugny, E. Van Vermaet (Eds.), Perspectives on Minority Influence, Cambridge University Press, Cambridge, UK, 1985.
[37] S. Galam, F. Jacobs, The role of inflexible minorities in the breaking of democratic opinion dynamics, Physica A 381 (2007) 366.
[38] J. Xie, S. Sreenivasan, G. Korniss, W. Zhang, C. Lim, B.K. Szymanski, Social consensus through the influence of committed minorities, Phys. Rev. E 84 (2011) 011130.
[39] D. Centola, The spread of behavior in an online social network experiment, Science 329 (2010) 1194.
[40] C. Castellano, M.A. Muñoz, R. Pastor-Satorras, Nonlinear q-voter model, Phys. Rev. E 80 (2009) 041129.
[41] P.S. Dodds, D.J. Watts, Universal behavior in a generalized model of contagion, Phys. Rev. Lett. 92 (2004) 218701.
[42] D. Volovik, S. Redner, Dynamics of confident voting, J. Stat. Mech. P04003 (2012).
[43] K. Suchecki, V.M. Equíluz, M. San Miguel, Conservation laws for the voter model in complex networks, Europhys. Lett. 69 (2004) 228.
[44] K. Suchecki, V.M. Equíluz, M. San Miguel, Voter model dynamics in complex networks: role of dimensionality, disorder, and degree distribution, Phys. Rev. E 72 (2005) 036132.
[45] C. Castellano, V. Loreto, A. Barrat, F. Cecconi, D. Parisi, Comparison of voter and Glauber ordering dynamics on networks, Phys. Rev. E 71 (2005) 066107.
[46] V. Sood, S. Redner, Voter model on heterogeneous graphs, Phys. Rev. Lett. 94 (2005) 178701.
[47] T. Antal, S. Redner, V. Sood, Evolutionary dynamics on degree-heterogeneous graphs, Phys. Rev. Lett. 96 (2006) 188104.
[48] V. Sood, T. Antal, S. Redner, Voter models on heterogeneous networks, Phys. Rev. E 77 (2008) 041121.
[49] F. Vazquez, V.M. Eguiluz, Analytical solution of the voter model on uncorrelated networks, New J. Phys. 10 (2008) 063011.
[50] M.J.A. Condorcet, Essai sur l'application de l'analyse à la probabilité des décisions rendues à la pluralité des voix, Imprimerie royale, Paris, France, 1785, facsimile edition, AMS Chelsea Publishing Series, vol. 252, New York, 1972.
[51] B. Grofman, G. Owen, S.L. Feld, Thirteen theorems in search of the truth, Theory Decis. 15 (1983) 261.
[52] R. Boyd, P.J. Richerson, The Origin and Evolution of Cultures, Oxford University Press, Oxford, UK, 2005.
[53] L. Conradt, C. List, Group decision making in humans and animals, Philos. Trans. R. Soc. Lond. B, Biol. Sci. 364 (2009) 719.
[54] V. Spirin, P.L. Krapivsky, S. Redner, Phys. Rev. E 63 (2001) 036118.
[55] V. Spirin, P.L. Krapivsky, S. Redner, Phys. Rev. E 65 (2001) 016119.
[56] S. Galam, Application of statistical physics to politics, Physica A 274 (1999) 132.
[57] K. Sznajd-Weron, J. Sznajd, Opinion evolution in closed community, Int. J. Mod. Phys. C 11 (2000) 1157.
[58] S. Galam, Minority opinion spreading in random geometry, Eur. Phys. J. B 25 (2002) 403.
[59] D. Stauffer, Monte Carlo simulations of Sznajd models, J. Artif. Soc. Soc. Simul. 5 (2002) 1.
[60] P.L. Krapivsky, S. Redner, Dynamics of majority rule in two-state interacting spin systems, Phys. Rev. Lett. 90 (2003) 238701.
[61] C.M. Bender, S.A. Orszag, Advanced Mathematical Methods for Scientists and Engineers, McGraw-Hill, New York, 1978.
[62] P. Chen, S. Redner, Majority rule dynamics in finite dimensions, Phys. Rev. E 71 (2005) 036101.
[63] R. Lambiotte, S. Redner, Dynamics of vacillating voters, J. Stat. Mech. L10001 (2007).
[64] R. Lambiotte, S. Redner, Dynamics of non-conservative voters, Europhys. Lett. 82 (2008) 18007.
[65] F. Slanina, K. Sznajd-Weron, P. Przybyła, Some new results on one-dimensional outflow dynamics, Europhys. Lett. 82 (2008) 18006.
[66] R. Lambiotte, S. Thurner, R. Hanel, Unanimity rule on networks, Phys. Rev. E 76 (2007) 046101.
[67] R.J. Glauber, Time-dependent statistics of the Ising model, J. Math. Phys. 4 (1963) 294.
[68] M. Mobilia, S. Redner, Majority versus minority dynamics: phase transition in an interacting two-state spin system, Phys. Rev. E 68 (2003) 046106.
[69] D. ben-Avraham, in: V. Privman (Ed.), Non-equilibrium Statistical Mechanics in One Dimension, Cambridge University Press, Cambridge, UK, 1997, Chap. 2.
[70] N. Claidière, A. Whiten, Integrating the study of conformity and culture in humans and nonhuman animals, Psychol. Bull. 138 (2012) 126.
[71] T.J.H. Morgan, K.N. Laland, The biological bases of conformity, Front. Neurosci. 6 (2012) 87.
[72] F. Vazquez, S. Redner, Ultimate fate of constrained voters, J. Phys. A 37 (2004) 8479.
[73] R. Axelrod, The dissemination of culture: a model with local convergence and global polarization, J. Confl. Resolut. 41 (1977) 203.
[74] R. Axtell, R. Axelrod, J. Epstein, M.D. Cohen, Aligning simulation models: a case study and results, Comput. Math. Organ. Theory 1 (1996) 123.
[75] R. Axelrod, The Complexity of Cooperation, Princeton University Press, Princeton, NJ, USA, 1997.
[76] C. Castellano, M. Marsili, A. Vespignani, Nonequilibrium phase transition in a model for social influence, Phys. Rev. Lett. 85 (2000) 3536.
[77] D. Vilone, A. Vespignani, C. Castellano, Ordering phase transition in the one-dimensional Axelrod model, Eur. Phys. J. B 30 (2002) 399.

Please cite this article in press as: S. Redner, Reality-inspired voter models: A mini-review, C. R. Physique (2019), https://doi.org/10.1016/j.crhy.2019.05.004

[78] K. Klemm, V.M. Eguiluz, R. Toral, M. San Miguel, Nonequilibrium transitions in complex networks: a model of social interaction, Phys. Rev. E 67 (2003) 026120.
[79] K. Klemm, V.M. Eguiluz, R. Toral, M. San Miguel, Global culture: a noise-induced transition in finite systems, Phys. Rev. E 67 (2003) 045101(R).
[80] F. Vazquez, S. Redner, Non-monotonicity and divergent time scale in Axelrod model dynamics, Europhys. Lett. 78 (2007) 18002.
[81] E.N. Lorenz, Deterministic nonperiodic flow, J. Atmos. Sci. 20 (1963) 130.
[82] R.M. May, W.J. Leonard, Nonlinear aspects of competition between three species, SIAM J. Appl. Math. 29 (1975) 243.
[83] See, e.g., A.S. Perelson, P.W. Nelson, Mathematical analysis of HIV-1 dynamics in vivo, SIAM Rev. 41 (1999) 3.
[84] G. Weisbuch, G. Deffuant, F. Amblard, J.P. Nadal, Meet, discuss, and segregate! Complexity 7 (2002) 55.
[85] R. Hegselmann, U. Krause, Opinion dynamics and bounded confidence models, analysis, and simulation, J. Artif. Soc. Soc. Simul. 5 (2002) 3.
[86] E. Ben-Naim, P.L. Krapivsky, S. Redner, Bifurcations and patterns in compromise processes, Physica D 183 (2003) 190.

Please cite this article in press as: S. Redner, Reality-inspired voter models: A mini-review, C. R. Physique (2019), https://doi.org/10.1016/j.crhy.2019.05.004